

# ChemComm

Accepted Manuscript



This is an *Accepted Manuscript*, which has been through the Royal Society of Chemistry peer review process and has been accepted for publication.

*Accepted Manuscripts* are published online shortly after acceptance, before technical editing, formatting and proof reading. Using this free service, authors can make their results available to the community, in citable form, before we publish the edited article. We will replace this *Accepted Manuscript* with the edited and formatted *Advance Article* as soon as it is available.

You can find more information about *Accepted Manuscripts* in the [Information for Authors](#).

Please note that technical editing may introduce minor changes to the text and/or graphics, which may alter content. The journal's standard [Terms & Conditions](#) and the [Ethical guidelines](#) still apply. In no event shall the Royal Society of Chemistry be held responsible for any errors or omissions in this *Accepted Manuscript* or any consequences arising from the use of any information it contains.

## COMMUNICATION

## A minimized designer protein for facile biofabrication of ZnS:Mn immuno-quantum dots

We haCite this: DOI:  
10.1039/x0xx00000x

Weibin Zhou, Brian J. F. Swift and François Baneyx\*<sup>c</sup>

Received 00th January 2012,  
Accepted 00th January 2012

DOI: 10.1039/x0xx00000x

www.rsc.org/

**A minimized protein consisting of a linear ZnS-binding peptide fused to an antibody-binding domain supports the one-step aqueous synthesis of Mn-doped ZnS nanocrystals that exhibit smaller size, brighter fluorescence and improved antibody-binding relative to those made with the original designer protein.**

The fabrication of protein-coated quantum dots (QDs) benign to human and the environment is a complex and time-consuming process that is further complicated by the inherent toxicity of commonly used core materials (e.g., CdSe) and by the need for polymer coatings and secondary functional groups<sup>1</sup> which can exert a deleterious effect on biological systems.<sup>3</sup> To circumvent these limitations, we previously built a “designer” protein that supports the aqueous and one-pot synthesis of undoped and manganese-doped ZnS QDs whose crystalline cores are approximately 4 nm in diameter.<sup>2, 4</sup> The 27-kDa BB-TrxA::CT43 fusion protein (Fig. 1A) consists of an antibody-binding domain derived from *S. aureus* protein A (BB) followed by a disulfide-constrained ZnS-binding peptide (CT43) inserted within the active site loop of *E. coli* Thioredoxin A (TrxA). BB-TrxA::CT43 prevents uncontrolled precipitation of ZnS (or ZnS:Mn) via CT43-dependent capping and allows for rapid production of immuno-QDs by BB-mediated conjugation of antibodies to protein-stabilized nanocrystals.<sup>2, 4</sup>

From a bio-imaging perspective, nanoparticles with small hydrodynamic diameters ( $D_h$ ) are preferable to larger ones because they are more efficiently transported to a variety of tissues and subcellular locations.<sup>5</sup> Small QDs ( $\leq 10$  nm) are also desirable from a toxicological standpoint because they are more readily cleared by the renal system.<sup>6</sup> For our biofabricated QDs, reducing  $D_h$  means decreasing the size of the designer protein without affecting its ability to stabilize nanocrystals. If antibody-binding functionality is to be maintained, this means truncating or eliminating the TrxA domain while repositioning the CT43 motif as a fusion to BB.

The CT43 dodecapeptide was identified as one of several ZnS binders from a screen of the FliTrx flagellar display library.<sup>4, 7</sup> In the original display system, and in the BB-TrxA::CT43 designer protein, CT43 is presented to the solvent in a disulfide-bonded loop that reduces its flexibility and available degrees of freedom (Fig. 1A). This has important consequences on inorganic binding since conversion from circular to linear topology often reduces or even entirely eliminates the ability of solid binding peptides (SBPs) to interact with their cognate materials.<sup>8</sup> For nucleation and growth processes, a decrease in affinity means less efficient capping and the production of larger particles.<sup>9</sup> On the other hand, certain disulfide-bonded SBPs are largely unaffected by linearization,<sup>8b, 8c</sup> and conversion of certain binders to a linear configuration has even been reported to increase inorganic affinity.<sup>10</sup>

To determine if an unconstrained version of CT43 would remain capable of supporting QD synthesis, we used site directed mutagenesis to convert the first and second cysteine of BB-TrxA::CT43 to serine. The resulting proteins, BB-TrxA::CT43-C32S and BB-TrxA::CT43-C35S (using the numbering system of native TrxA) were purified to homogeneity along with the wild type and proteins were used at a 5  $\mu$ M concentration to synthesize ZnS:Mn QDs by dropwise addition of sodium sulfite to a precursor solution of zinc and manganese.<sup>2</sup> After 5 days of aging at 37°C, all solutions were bright orange under UV illumination and  $D_h$  measured by dynamic light scattering were comparable for all suspensions (~15 nm). Nevertheless, maximum emission intensities at 590 nm, a wavelength characteristic of the  ${}^4T_1 \rightarrow {}^6A_1$  Mn<sup>2+</sup> transition, were 10% and 16% lower when the C32S or C35S variant (respectively) was used in place of the wild type. We conclude that although the disulfide-bonded conformation of CT43 is not required for efficient QD biofabrication, it exerts a small positive impact on optical properties.

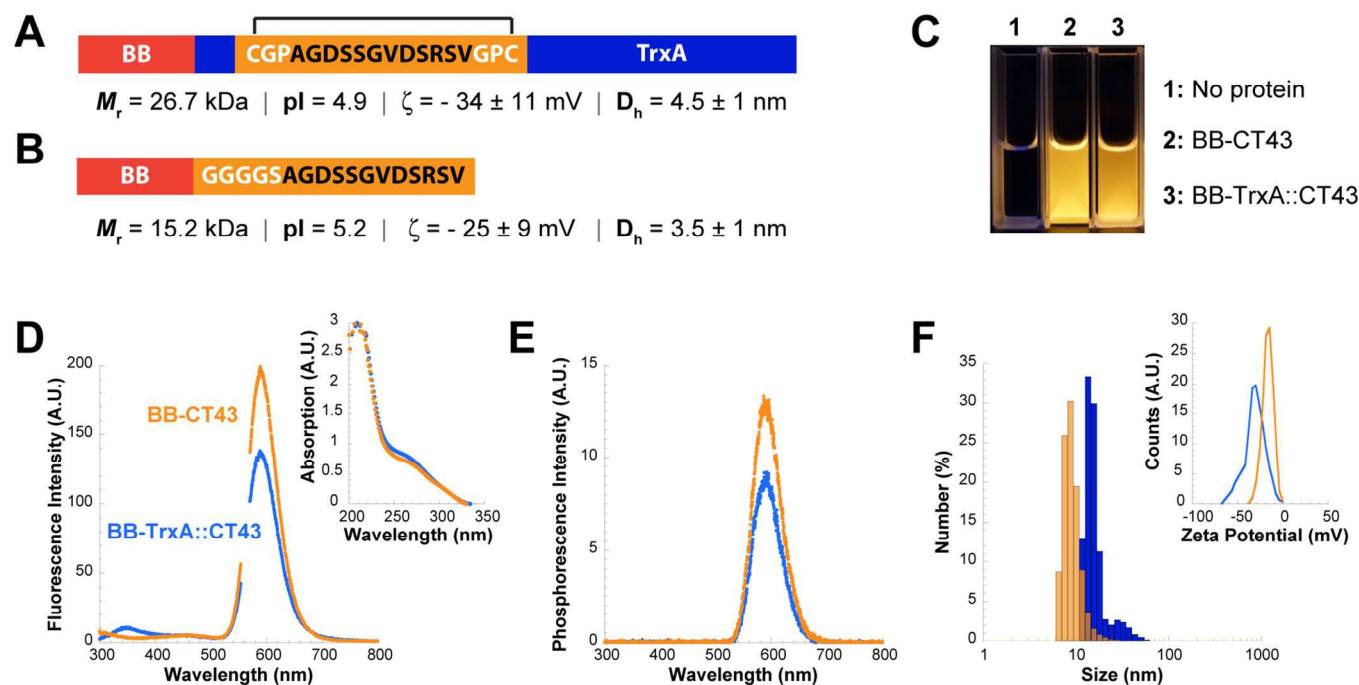


**Figure 1:** Comparison of the properties of ZnS:Mn nanocrystals biofabricated with the BB-TrxA::CT43 and BB-CT43 designer proteins. Schematic structures of BB-TrxA::CT43 (A) and BB-CT43 (B). The antibody-binding BB domain is in red, TrxA in blue and the ZnS-binding region in orange. The amino acid sequence of the CT43 peptide is in black and invariant tripeptides (A) or flexible linker (B) in white using the one letter code. The disulfide bond between cysteine residues is shown in the case of BB-TrxA::CT43. Calculated molecular mass and pI, and measured zeta potential and hydrodynamic diameters for the purified proteins are shown below sketches. (C) Appearance of ZnS:Mn nanocrystals fabricated with 5  $\mu$ M of BB-CT43 or BB-TrxA::CT43 under UV illumination. (D) Fluorescence emission spectra of nanocrystals produced with BB-CT43 (orange) or BB-TrxA::CT43 (blue) after excitation at 280 nm. The inset shows the corresponding absorption spectra. (E) Phosphorescence emission spectra after excitation at 280 nm. (F) Distribution of hydrodynamic diameters for nanocrystals produced with BB-CT43 (orange) or BB-TrxA::CT43 (blue). The inset shows the corresponding zeta potentials.

Based on the above findings, we fused a linear version of the CT43 sequence to the C-terminus of BB via a flexible linker, completely eliminating TrxA in the process (Fig. 1B). As expected, the resulting protein (BB-CT43) supported the production of ZnS:Mn QDs (Fig. 1C). More surprisingly, while the absorption spectra of the two colloidal suspensions were comparable (Fig. 1D, inset), QDs fabricated with BB-CT43 exhibited 30% higher emission intensity at 590 nm relative to particles made with BB-TrxA::CT43 (Fig. 1D). Inductively coupled atomic emission spectroscopy (ICP-AES) ruled out the possibility that this was due to a change in Mn incorporation. Rather, we attribute the improvement to the absence of the TrxA domain since room temperature phosphorescence measurements, which are sensitive to the nature of adsorbates,<sup>12</sup> show that BB-CT43-stabilized nanocrystals experience less quenching compared to those produced with BB-TrxA::CT43 (Fig. 1E). Quantum yields calculated as before<sup>4</sup> were 6.5% and 7.5% for QDs fabricated with BB-TrxA::CT43 and BB-CT43, respectively.

Consistent with the fact that elimination of TrxA yields a protein that is 25% more compact than its parent (Fig. 1A-B), the mean  $D_h$  of particles biofabricated with BB-CT43 was  $9.5 \pm 2$  nm compared to  $15 \pm 3$  nm for BB-TrxA::CT43-stabilized nanocrystals (Fig. 1F). Also as expected from the lower zeta potential ( $\zeta$ ) of BB-CT43 (Fig. 1A-B), QDs made with the minimized protein had a  $\zeta$  of  $-16.5 \pm 6$  mV relative to  $-30 \pm 10$  mV for particles produced with the full-length protein (Fig. 1F). This change in charge did not affect colloidal stability. BB-CT43-capped QDs retained their optical properties over months of storage at 4 $^{\circ}$  C and did not aggregate or

experience significant fluorescence loss when exposed to pH ranging from 7 and 9 and salt concentrations as high as 500 mM NaCl (Fig. 2). Additionally, there was no significant change in colloidal or optical properties following one week of incubation under physiological conditions (37 $^{\circ}$ C, 150 mM NaCl). It is therefore likely that steric exclusion effects play an important role in particle stabilization.<sup>13</sup> On the other hand, BB-CT43-stabilized nanocrystals were sensitive to acidification (Fig. 2), just like particles produced with BB-TrxA::CT43.<sup>2</sup>

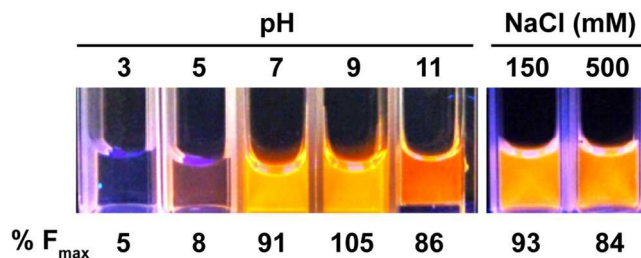


**Figure 2:** Stability of ZnS:Mn nanocrystals fabricated with BB-CT43. Colloidal suspensions were photographed under UV illumination 1h after pH adjustment with 0.1 M HCl or NaOH, or after addition of the indicated NaCl concentration. Numbers below samples correspond to the ratio of maximum fluorescence intensity at 590 nm ( $\lambda_{ex} = 280$  nm) to that of a control QD solution synthesized at the standard pH of 8.2.

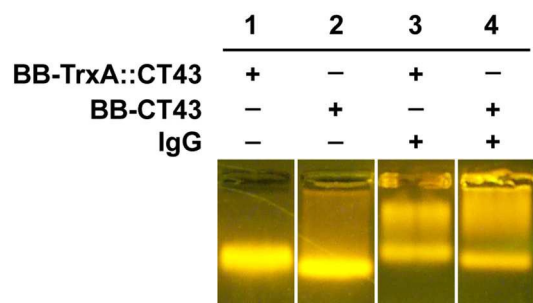


**Figure 3:** Production of immuno-QDs. ZnS:Mn nanocrystals fabricated with 5  $\mu$ M of BB-TrxA::CT43 or BB-CT43 were fractionated on a 0.75% agarose gel in the absence of additive (lanes 1 and 2) or after 1h incubation with 1  $\mu$ M human IgG (lanes 3 and 4).<sup>2</sup>

To demonstrate that the BB domain of the minimized protein was functional for antibody binding, QDs fabricated with BB-TrxA::CT43 or BB-CT43 were fractionated on 0.75% agarose gels.<sup>2, 4</sup> In the absence of additive, both colloidal suspensions migrated as tight bands (Fig. 3) with BB-CT43-stabilized QDs traveling closer to the cathode (at the bottom of the gel) due to their smaller  $D_h$ . Incubation with human immunoglobulin G (IgG) at a 1:5 molar ratio of antibody to designer protein led to a decrease in the intensities of these bands and to the concomitant appearance of fluorescent material migrating closer to the loading wells (lanes 2 and 3). These species, which correspond to antibody-derivatized QDs,<sup>2</sup> accounted for 60% of the total fluorescence for QDs made with BB-TrxA::CT43 and 70% of the total fluorescence for nanocrystals produced with BB-CT43. Thus, antibody decoration is slightly more efficient with BB-CT43-stabilized QDs, perhaps because the BB domain is more accessible to the solvent. In support of this hypothesis, BB-CT43-based immuno-QDs migrated over a broader range of positions compared to those produced with BB-TrxA::CT43, which suggests that they are decorated with different numbers of antibodies (we previously calculated that 5 to 6 designer protein molecule stabilize each nanocrystals which means that up to 6 antibody molecules might bind to a QD).<sup>2</sup>

In summary, we have shown that a minimal version of BB-TrxA::CT43 consisting of the *S. aureus* BB antibody binding domain fused to a linear version of CT43 remains functional for the facile biofabrication of luminescent ZnS:Mn nanocrystals. QDs produced with the minimized protein are as stable as those made with BB-TrxA::CT43, but 30% brighter and more accessible for antibody binding. A one-third reduction in  $D_h$  should make these optical probes more versatile and less toxic for biological imaging applications.

This work was supported by NIH award 1U19ES019545-01 from the National Institute of Environmental Health Sciences.

## Notes and references

<sup>a</sup> Department of Chemical Engineering, University of Washington, Box 351750, Seattle, WA 98195-1750

† Electronic Supplementary Information (ESI) available: Materials and methods See DOI: 10.1039/c000000x/

1(a) V. Biju, T. Itoh, A. Anas, A. Sujith and M. Ishikawa, *Anal. Bioanal. Chem.*, 2008, **391**, 2469; (b) T. Jamieson, R. Bakhshi, D. Petrova, R. Pocock, M. Imani and A. M. Seifalian,

*Biomaterials*, 2007, **28**, 4717; (c) I. L. Medintz, H. T. Uyeda, E. R. Goldman and H. Mattoussi, *Nat. Mater.*, 2005, **4**, 435; (d) F. M. Winnik and D. Maysinger, *Acc Chem Res*, 2013, **46**, 672.

2 W. Zhou and F. Baneyx, *ACS Nano*, 2011, **5**, 8013.

3 A. Shiohara, S. Hanada, S. Prabakar, K. Fujioka, T. H. Lim, K. Yamamoto, P. T. Northcote and R. D. Tilley, *J Am Chem Soc*, 2010, **132**, 248.

4 W. Zhou, D. T. Schwartz and F. Baneyx, *J. Am. Chem. Soc.*, 2010, **132**, 4731.

5 E. Oh, J. B. Delehanty, K. E. Sapsford, K. Susumu, R. Goswami, J. B. Blanco-Canosa, P. E. Dawson, J. Granek, M. Shoff, Q. Zhang, P. L. Goering, A. Huston and I. L. Medintz, *ACS Nano*, 2011, **5**, 6434.

6 H. S. Choi, W. Liu, P. Misra, E. Tanaka, J. P. Zimmer, B. I. Ipe, M. G. Bawendi and J. V. Frangioni, *Nat. Biotechnol.*, 2007, **25**, 1165.

7 Z. Lu, K. S. Murray, V. Van Cleave, E. R. LaVallie, M. L. Stahl and J. M. McCoy, *Biotechnology*, 1995, **13**, 366.

8(a) W. S. Choe, M. S. R. Sastry, C. K. Thai, H. Dai, D. T. Schwartz and F. Baneyx, *Langmuir*, 2007, **23**, 11347; (b) M. Hnilova, E. E. Oren, U. O. S. Seker, B. R. Wilson, S. Collino, J. S. Evans, C. Tamerler and M. Sarikaya, *Langmuir*, 2008, **24**, 12440; (c) U. O. S. Seker, B. Wilson, S. Dincer, I. W. Kim, E. E. Oren, J. S. Evans, C. Tamerler and M. Sarikaya, *Langmuir*, 2007, **23**, 7895.

9(a) D. Chiu, W. Zhou, S. Kitayaporn, D. T. Schwartz, K. Murali-Krishna, T. J. Kavanagh and F. Baneyx, *Bioconjug. Chem.*, 2012, **23**, 610; (b) W. Zhou and F. Baneyx, *Biochem. Eng. J.*, 2014, **89**, 28.

10 H. B. Chen, X. D. Su, K.-G. Neoh and W. S. Choe, *Langmuir*, 2009, **25**, 1588.